DOI: 10.1002/ejic.200601059

Zinc, Cadmium and Mercury Dithiocarboxylates: Synthesis, Characterization, Structure and Their Transformation to Metal Sulfide Nanoparticles

Gotluru Kedarnath,[a] Vimal K. Jain,*[a] Shamik Ghoshal,[a] Gautam K. Dey,[b] Carol A. Ellis,[c] and Edward R. T. Tiekink*[c]

Keywords: Zinc / Cadmium / Mercury / Dithiocarboxylates / Nanoparticles

Reactions of $M(OAc)_2{\cdot}nH_2O$ and $M(OAc)_2$(tmeda) with dithiocarboxylic acids gave $[M(S_2CTol)_2]_n$ (**1**) (M = Zn or Cd; Tol = C_6H_4Me-4) and $[M(S_2CAr)_2(tmeda)]$ (**3**) (M = Zn, Cd, Hg; Ar = Ph or Tol), respectively, in high yields as deep-colored crystalline solids. The former are soluble in pyridine to give pyridine adducts $[M(S_2CTol)_2(py)]$ (**2**). These complexes were characterized by elemental analysis, UV/Vis and NMR (^1H, ^{13}C) spectroscopy. The absorptions in the electronic spectra have been assigned to ligand-to-ligand charge-transfer transitions. The crystal and molecular structures of the monomeric species $[Zn(S_2CTol)_2(py)]$ (**2**), $[Zn(S_2CPh)_2(tmeda)]$ (**3a**), $[Zn(S_2CTol)_2(tmeda)]$ (**3b**) and $[Cd(S_2CTol)_2(tmeda)]$ (**3d**) have been established by X-ray crystallography. In $[Zn(S_2CTol)_2(py)]$, chelating dithiocarboxylate ligands and pyridine define a coordination geometry intermediate between square pyramidal and trigonal bipyramidal. In each of **3a** and **3b**, tetrahedral N_2S_2 coordination geometries are found as the dithiocarboxylate ligands are effectively monodentate; evidence for the greater coordination potential is found for $^-S_2CTol$ over ^-S_2CPh. Chelating dithiocarboxylate ligands in $[Cd(S_2CTol)_2(tmeda)]$ (**3d**) lead to an octahedral geometry. Thermal behavior has been studied by thermogravimetric analysis. The $[M(S_2CAr)_2(tmeda)]$ complexes underwent a three-step decomposition. Pyrolysis in the temperature range 300–500 °C and solvothermal decomposition in ethylenediamine and hexadecylamine (HDA) gave metal sulfide nanoparticles. The MS (M = Zn, Cd, Hg) nanoparticles were characterized by XRD, EDAX, absorption/emission spectroscopy and electron microscopy (TEM). Solvothermal decomposition gave hexagonal phases of nanoparticles whereas heating in a furnace gave cubic ZnS and HgS, and hexagonal CdS.

Introduction

During the past two decades considerable effort has been made to prepare high-quality monodispersed surface-passivated nanoparticles of II–VI semiconductors.[1] Owing to their quantum-confinement effect, semiconductor nanoparticles exhibit remarkable size- and shape-dependent optical properties which have led to their use in opto-electronic devices[2–6] and biological imaging.[7,8] Although a wide range of synthetic routes have been developed to prepare II–VI semiconductor nanoparticles,[8–11] decomposition of single-source molecular precursors in a suitable solvent has proved quite successful for isolation of high-quality nanoparticles within a narrow size distribution. The area has been dominated by ZnE and CdE (E = S, Se, Te) nanoparticles with limited investigations on HgE. Metal organochalcogenolates, $[M(EPh)_2(tmeda)]$ (M = Zn or Cd; E = S, Se or Te),[12] thiocarboxylates $[M(SCOR)_2L_2]$ (M = Zn or Cd; L = tmeda, 2-lutidene; R = Me, *t*Bu)[13] and $[Cd(SCOPh)_2(2,2'\text{-bipyridine})]$,[14] selenocarboxylates, $[M(SeCOAr)_2(tmeda)]$ (M = Zn or Cd),[15] xanthates $[M(S_2COR)_2]$ (M = Zn or Cd; R = Et, *i*Pr),[16,17] dithiocarbamates $[M(S_2NRR')_2]$ (M = Zn or Cd)[18,19] and dithiophosphinates $[M(S_2P\textit{i}Bu_2)_2]$ (M = Zn, Cd)[20] have been employed for the preparation of ME (M = Zn, Cd; E = S, Se, Te) nanoparticles/thin films.

Chemistry of the zinc-triad 1,1-dithiolates has been of considerable interest due to their numerous applications (e.g., lubricating oil in combustion engine, vulcanization of rubber, floating agents in metallurgy) and diverse structural features.[21–24] Subtle changes in organic substituents on the dithiolate group or in an auxiliary ligand often result in different structural motifs. Thus, molecules with zero- (discrete mono- and bi-nuclear complexes), one-, two- and three-dimensional structural motifs have been isolated and structurally characterized.[24] The 1,1-dithiolate chemistry of the zinc-triad has been dominated by ligands of the type **A**–**D** with relatively little attention to dithiocarboxylates (**E**), Scheme 1.[25–27] With the above in mind, it was consid-

[a] Chemistry Division, Bhabha Atomic Research Centre, Mumbai 400085, India
E-mail: jainvk@apsara.barc.ernet.in
[b] Materials Science Division, Bhabha Atomic Research Centre, Mumbai 400085, India
[c] Department of Chemistry, The University of Texas at San Antonio, One UTSA Circle, Texas 78249–0698, USA
E-mail:Edward.Tiekink@utsa.edu

Supporting information for this article is available on the WWW under http://www.eurjic.org or from the author.

ered worthwhile to explore the dithiocarboxylate chemistry of zinc, cadmium and mercury with the aim of isolating new structural motifs and also to develop a new family of promising single-source molecular precursors for the synthesis of MS nanoparticles. Results of this work are described herein.

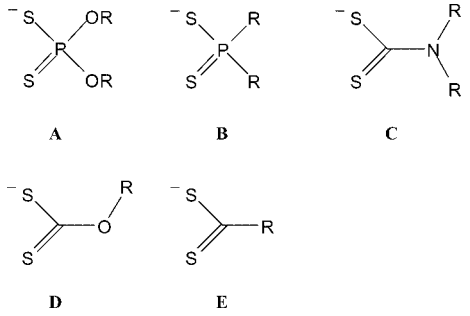

Scheme 1.

Results and Discussion

Treatment of $M(OAc)_2 \cdot 2H_2O$ with *p*-tolyldithiocarboxylic acid in methanol gave sparingly soluble orange complexes of composition $[M(S_2Ctol)_2]$ (**1**) [M = Zn (**1a**) or Cd (**1b**)]. The complexes dissolved readily in pyridine solution, with concomitant formation of the corresponding pyridine adducts $[Zn(S_2CTol)_2(py)]$ (**2**). The reaction of $[M(OAc)_2$-(tmeda)] with dithiocarboxylic acid in benzene afforded deep-colored complexes of the general formula, $[M(S_2COAr)_2(tmeda)]$ (**3**) [Equation (1)].

$$[M(OAc)_2(tmeda)] + 2\ ArCS_2H \rightarrow [M(S_2CAr)_2(tmeda)] + 2\ AcOH\ldots \quad (1)$$

3

M	Ar	
Zn	Ph	**3a**
Zn	Tol	**3b**
Cd	Ph	**3c**
Cd	Tol	**3d**
Hg	Ph	**3e**
Hg	Tol	**3f**

The electronic spectra of these complexes in dichloromethane solution displayed two (Ar = Ph) and three (Ar = Tol) absorption bands and are assigned for transitions in thiocarbonyl group. The electronic spectra of metal dithiocarboxylates have been reported to display characteristic absorption maxima in the region 250–550 nm attributable to π–π* and n–π* transitions.[28] The ^1H NMR spectra exhibited characteristic peaks due to tmeda and dithiolate ligand protons. The absence of singlets ascribed to the SH proton in the spectra indicate deprotonation of the acid. The NMe_2 and NCH_2 protons resonances appeared as singlets in the ranges 2.39–2.65 and 2.57–2.73 ppm, respectively. The resonance due to 2,6-protons of the aryl ring are deshielded with reference to the free ligand. The $^{13}C\{^1H\}$ NMR spectra showed singlets for NMe_2 and NCH_2 carbon atoms of tmeda at ca. 46.0 ppm and ca. 56.5 ppm, respectively. The resonance due to thiocarbonyl carbon (C=S) is deshielded (<20 ppm) on complexation, deshielding being greater in cadmium complexes than the corresponding zinc derivatives.

Structural Characteristics

The molecular structure of $[Zn(S_2CTol)_2(py)]$ (**2**) is represented in Figure 1 (a). The molecule is disposed about a crystallographic twofold axis which bisects the pyridine molecule and contains the zinc atom. The zinc atom is five-coordinate within a NS_4 donor set defined by two asymmetrically chelating dithiocarboxylate ligands and the pyridine-N atom. The Zn–S1 and Zn–S2 bond lengths are 2.3499(9) and 2.6046(11) Å, respectively and this asymmetry is reflected in the associated C–S distances so that S1–C1 is significantly longer than S2–C2, i.e., 1.716(3) and 1.679(3) Å,

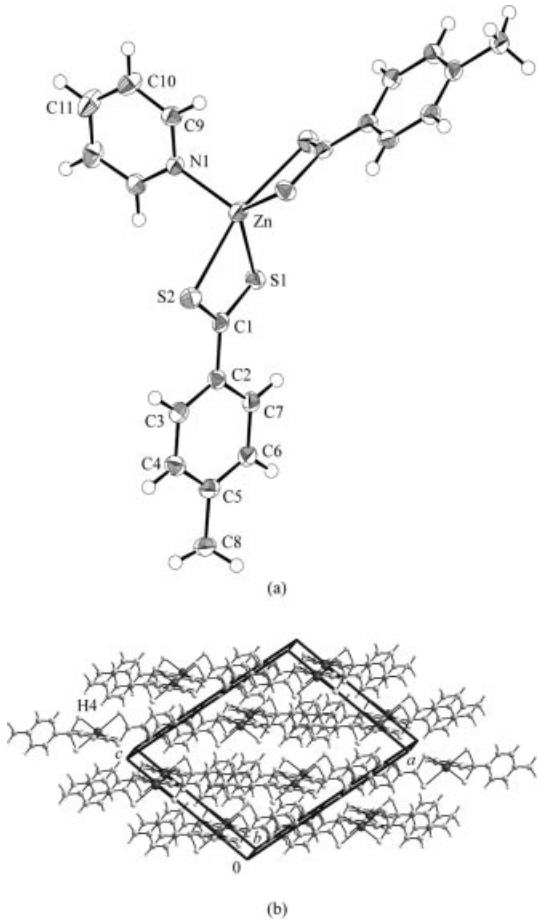

Figure 1. (a) Molecular structure and (b) unit cell contents for $[Zn(S_2CTol)_2(py)]$ (**2**).

respectively; the Zn–N1 distance is 2.046(3) Å. The dihedral angle between the two ZnS_2C chelate rings is 53.96(7)° and each of these is effectively orthogonal to the pyridine ring, dihedral angle = 79.87(10)°. The range of angles subtended at the zinc atom extends from 72.04(2)°, for the S1–Zn–S2 chelate angle to 164.55(4)°, for S2–Zn–S2^{i}; symmetry operation *i*: *–x*, *y*, 1/2 – *z*. The coordination geometry is intermediate between square pyramidal (τ = 0) and trigonal bipyramidal (τ = 1) as exemplified in the value of τ of 0.61.[29] The closely related structure of [Zn($S_2CC_6H_2$-4-OH-3,5-tBu$_2$)$_2$(py)][26] also features an intermediate geometry but one more inclined towards a square-pyramidal geometry as judged by the τ value of 0.43. The 1,1-dithiolate ligand is not strictly planar, there being a twist about the C1–C2 bond in **2** as seen in the value of –162.7(2)° for the S1/C1/C2/C3 torsion angle. In the crystal structure, Figure 1 (b), molecules pack in layers along (101). The primary contacts within layers are π···π interactions of 3.7202(19) Å between interdigitated C2–C7 rings (symmetry operation: 1/2 – *x*, 1/2 – *y*, *–z*). The interactions between successive layers are of the type C–H···π. Thus, the C4–H···ring centroid (pyridine) distance is 2.88 Å with an angle of 153° subtended at the H4 atom (symmetry operation: 1/2 + *x*, 1/2 + *y*, *z*).

A formal decrease in the coordination number of zinc is found in the structure of [Zn(S_2CTol)$_2$(tmeda)] (**3b**). The molecule, Figure 2 (a), has twofold symmetry, with the axis bisecting the tmeda ligand and containing zinc atom. The zinc atom is four-coordinate with the N_2S_2 coordination geometry defined by chelating tmeda and monodentate dithiocarboxylate ligands. The respective Zn–S1 and Zn–S2 distances are 2.3238(7) and 3.0860(9) Å, and these distances are significantly shorter and longer than the equivalent distances in the pyridine analog, respectively. The asymmetric mode of coordination is reflected in the respective S1–C1 and S2–C1 bond lengths of 1.705(3) and 1.667(3) Å; the Zn–N1 distance is 2.170(2) Å. The range of angles subtended at the tetrahedrally coordinated zinc atom is 84.11(11)°, for the N1–Zn–N1^{i} chelate angle, to 132.46(5)° for S1–Zn–S1^{i}; symmetry operation *i*: *–1 – x*, *–y*, *z*. The wider angle is certainly due to the close approach of the S2 atoms. A small twist is apparent between the S_2C and aromatic ring as seen in the S1/C1/C2/C3 torsion angle of 174.88(18)°. In the crystal structure, Figure 2 (b), the molecules form chains along the *c* axis stabilized by C_{methyl}–H···π interactions so that the C8–H···ring centroid of C2–C7 distance is 2.88 Å and angle at H of 130° for symmetry operation: –1/2 – *x*, *y*, –1/2 + *z*.

The influence of substituting the $^{-}S_2$CTol ligand by $^{-}S_2$CPh was investigated by examining the crystal and molecular structure of [Zn(S_2CPh)$_2$(tmeda)] (**3a**). The molecule, Figure 3 (a), has twofold symmetry as described for **3b** but the structures are not isomorphous. To a first approximation, the coordination geometry for both structures is the same. Thus, the zinc atom exists is a distorted tetrahedral geometry defined by a N_2S_2 donor set. The Zn–S1 and Zn–S2 distances of 2.3079(12) and 3.2736(14) Å are respectively, shorter and longer than the comparable distances in **3b**. This is reflected in the S1–C1 and S2–C1 distances of

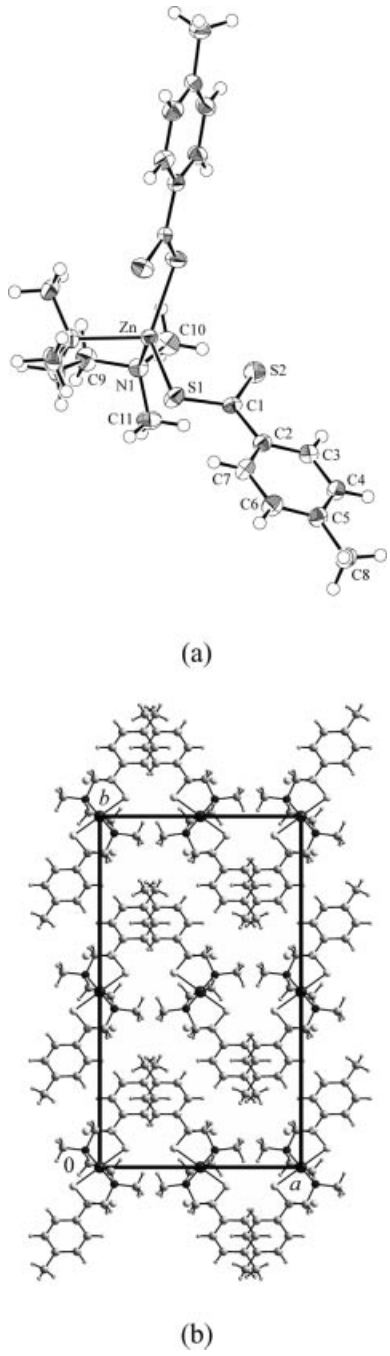

Figure 2. (a) Molecular structure and (b) unit cell contents for [Zn(S_2CTol)$_2$(tmeda)] (**3b**).

1.725(5) and 1.653(5) Å. The difference in mode of coordination of the two 1,1-dithiolate ligands can be conveniently realized by considering the Δ(Zn–S) and the associated Δ(C–S) values, with greater values been correlated with greater asymmetry. Thus, in **3b** these compute to 0.76 and 0.04 Å, respectively, which are smaller than the values found for **4a** of 0.97 and 0.07 Å, respectively. Further, the Zn–N1 distance of 2.127(4) Å is shorter in the present structure. These results correlate in the expected fashion with the electron-donating ability of the methyl group in the $^{-}S_2$CTol ligand that makes this a comparatively better

chelating agent. However, it is noted that there is a significant twist about the C1–C2 bond of the $^{-}S_2CTol$ ligand as seen in the value of 142.8(4)° for the S1/C1/C2/C3 torsion angle, and so the negative inductive effect exerted by the methyl group is not the reason for the different coordinating abilities. By contrast to the previously described crystal structures, in the absence of π···π and C–H···π interactions, C–H···S interactions dominate the crystal packing in **3a**. Thus, in addition to a variety of intramolecular C–H···S interactions, three intermolecular C–H···S interactions may be discerned in the stabilization of the crystal structure. A view of the unit-cell contents is shown in Figure 3 (b). Here, two C–H···S interactions are highlighted and show adjacent C–H atoms of an aromatic ring bridging S1 and S2 atoms of different ligands but of the same molecule. The parameters associated with interaction "(a)" are C6–H···S1^{i} of 3.10 Å with an angle of 164° subtended at the H6 atom, and "(b)" C5–H···S2^{ii} of 3.06 Å and angle 125°; symmetry operations *i*: *–x*, 1 – *y*, 1 – *z* and *ii*: *x*, 1 – *y*, –1/2 + *z*. Orthogonal C8–H···S2^{iii} interactions, i.e., involving methylene-H atoms, of 3.02 Å and angle 173°, link translationally related molecules along the *b*-direction into chains; symmetry operation *iii*: *x*, 1 + *y*, *z*.

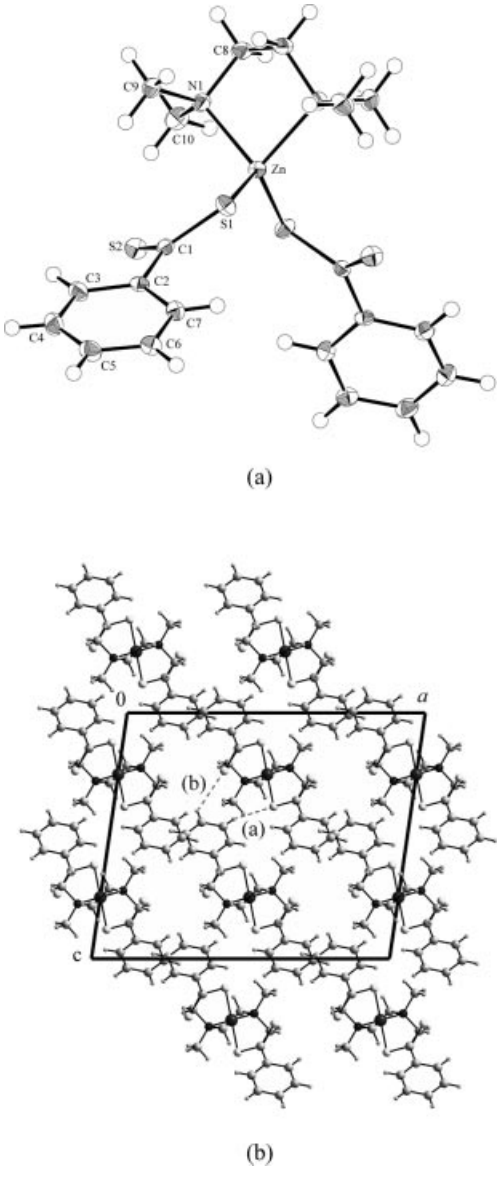

Figure 3. (a) Molecular structure and (b) unit cell contents for [Zn(S_2CPh)$_2$(tmeda)] (**3a**).

The remaining structure to be described is that of [Cd(S_2CTol)$_2$(tmeda)] (**3d**), shown in Figure 4. This structure is isomorphous with the zinc analog described above, but the coordination geometry is different. Here, owing to the greater propensity of the larger cadmium atom to increase its coordination number, the coordination geometry is based on a distorted octahedron within a N_2S_4 donor set. The dithiocarboxylate ligand forms nearly symmetric Cd–S bonds of 2.6508(8) and 2.7336(9) Å, Δ(Cd–S) is only 0.08 Å; the Cd–N1 bond length is 2.416(2) Å. Distortions from the ideal octahedral geometry may be traced to the acute chelate angles of 66.18(2)°, for S1–Cd–S2, and 76.15(12)°, for N1–Cd–N1^{i}; symmetry operation *i*: *–x*, *–y*, *z*. The CS_2 and aromatic portions of the 1,1-dithiolate ligand are effectively co-planar as evidenced by the S1/C1/C2/C3 torsion angle of –174.3(2)°. The crystal packing is as described above for **3d** with a C8–H···ring centroid of C2–C7 distance is 2.94 Å and angle at H of 131° for symmetry operation: –1/2 – *x*, *y*, 1/2 + *z*.

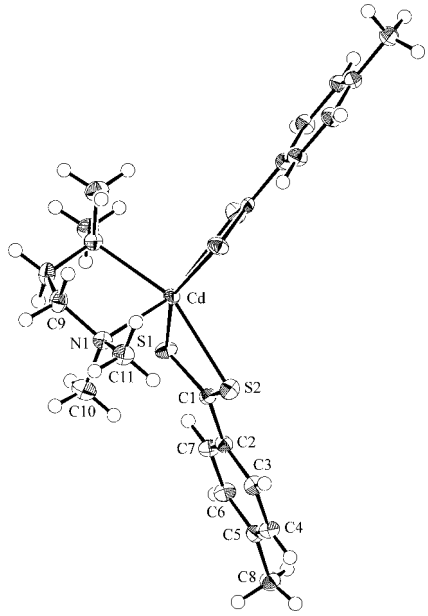

Figure 4. Molecular structure of [Cd(S_2CTol)$_2$(tmeda)] (**3d**).

Thermal Studies

TG analyses were carried out to study the thermal behavior and suitability of these complexes for the preparation of metal sulfides. These complexes underwent a three-step decomposition, exemplified for [Zn(S_2CPh)$_2$(tmeda)] (**3a**) in Figure S1 (see Supporting Information), with the formation of metal sulfides as inferred from the weight loss (e.g. **3a**, calculated weight loss: 80.0% and observed weight loss:

76.5%) and confirmed from the XRD patterns of the residues. The onset temperatures are **3a**, 194 °C; **3b**, 178 °C; **3c**, 175 °C; **3d**, 180 °C. The TG curves of the zinc complexes showed slightly separated steps while for the cadmium and mercury derivatives they were poorly resolved indicating instability of the intermediate species. The first step, based on percentage of weight loss (e.g. **3a**, calcd. weight loss for tmeda: 23.8% and obsd. weight loss for first step: 23.8%) has been attributed to the elimination of tmeda. The second and third steps can be characterized for decomposition of dithiocarboxylate groups.

Pyrolysis of $[M(S_2CAr)_2(tmeda)]$ (Ar = Ph, Tol) was carried out at 350 °C under flowing nitrogen for 2 h. In each case metal sulfides (MS; M = Zn, Cd, Hg) were formed as confirmed by their XRD patterns (see Figure 5 and Figures S2–S3 in the Supporting Information) and EDAX analysis (Ar = Ph) (ZnS: calcd 67.1, S 32.9; found Zn 60.2, S 39.8. CdS: calcd Cd 77.8, S 22.2; found Cd 74.3, S 25.7. HgS: calcd. Hg 86.2, S 13.8; found Hg 84.2, S 15.8). The XRD patterns of ZnS and HgS were consistent with the formation of cubic phase of the material,[30,31] whereas CdS was isolated in the hexagonal phase.[32] The pyrolysis of $[Cd(S_2CPh)_2(tmeda)]$ (**3c**), carried out at 300, 400 and 500 °C, also gave hexagonal CdS with the average particle sizes of 18, 36 and 43 nm, respectively, from the Scherrer equation.[33] This indicates that particle size increases with increasing decomposition temperature at a given time. The absorption spectrum of CdS nanoparticles (obtained at 300 °C) showed a broad peak at 505 nm. The emission profile displayed a band at 521 nm, which may be due to surface traps (Figure 6). The particles are of 15 nm in size as estimated from the Brus expression.[34]

Solvothermal decomposition of $[M(S_2CPh)_2(tmeda)]$ (M = Zn, Cd, Hg) was examined in different coordinating solvents, such as ethylenediamine and HDA, to assess their suitability as precursors for the preparation of MS nanoparticles. Pyrolysis of $[M(S_2CPh)_2(tmeda)]$ in refluxing ethylenediamine gave hexagonal phases of MS (from XRD) nanoparticles which were isolated as cream (ZnS), yellow-orange (CdS) and orange (HgS) powders by centrifugation (Figure S4 in the Supporting Information). The particle sizes, estimated from the Scherrer formula,[33] are 34 (ZnS), 29 (CdS) and 103 (HgS) nm. The mercury complex can be pyrolyzed in ethylenediamine at a temperature as low as 57 °C with the formation of hexagonal HgS, having an average particle size (diameter) of 21 nm. The absorption spectra of CdS and HgS nanoparticles (obtained at 122 °C in ethylenediamine) displayed peaks at 480 and 401 nm, respectively. Emission profile (Figure 7) of these CdS nanoparticles exhibited a band at 518 nm (bulk CdS bandgap is 515 nm), which may be due to surface traps.

Nanoparticles prepared under different conditions are known to give different phases and sizes due to different nucleation mechanisms.[35] It is likely that in the present circumstances different nanoparticles are obtained owing to different mechanisms of formation and temperatures. Thus, when the precursor is heated without solvent, initially tmeda is released (as inferred from TG curve) followed by decomposition of the complex, whereas in a coordinating solvent, the coordinating ligand helps in passivating the surface of the particles resulting in different phases.

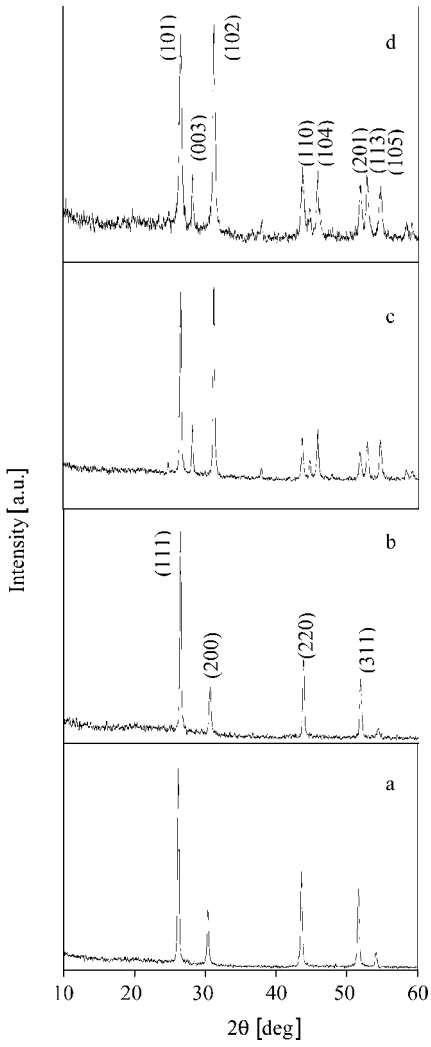

Figure 5. XRD patterns of the HgS nanoparticles prepared under different conditions from $[Hg(SC_2Ph)_2(tmeda)]$; a) heated in a furnace at 250 °C, b) heated in a furnace at 350 °C, c) thermolysis in ethylenediamine at 125 °C and d) thermolysis in HDA at 125 °C.

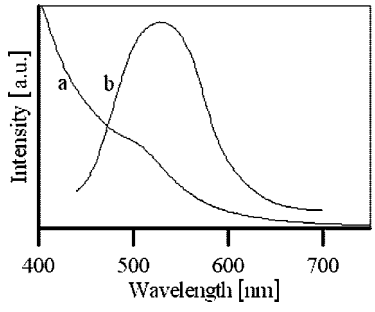

Figure 6. a) Absorption and b) emission spectra of CdS nanoparticles obtained by the pyrolysis of $[Cd(S_2CPh)_2(tmeda)]$ in a furnace at 300 °C under flowing nitrogen.

Pyrolysis of $[Cd(S_2CPh)_2(tmeda)]$ (**3c**) and $[Hg(S_2CPh)_2(tmeda)]$ (**3e**) was also carried out in HDA either at different

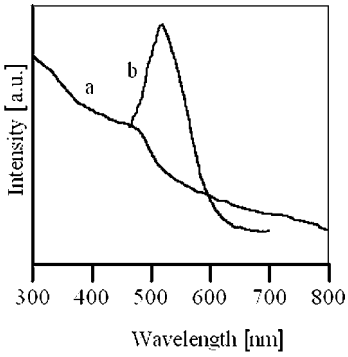

Figure 7. a) Absorption and b) emission spectra of CdS nanoparticles obtained by pyrolysis of $[Cd(S_2CPh)_2(tmeda)]$ in ethylenediamine at 122 °C.

temperatures and/or different concentrations of the precursor. Thermolysis of **3c** in HDA at 188, 188, and 225 °C having precursor/solvent mol ratio of 1:34, 1:55, and 1:55, respectively gave yellow-orange nanoparticles of hexagonal CdS with particle sizes 17, 26, and 34 nm, respectively. Their absorption spectra (Figure 8) in toluene showed exciton peaks at 466, 473 and 503 nm, respectively, which are blue shifted from bulk CdS (515 nm). The emission spectra of the samples prepared at 188 °C of precursor: solvent mol ratio of 1:34 and 1:55 exhibited a broad emission at 523 and 546 nm, respectively. Both absorption and emission maxima are red-shifted with increasing size of the CdS nanoparticles. Pyrolysis of **3e** in HDA (precursor/HDA mol ratio = 1:70) at 125 °C afforded the hexagonal phase of HgS,[36] whereas at 160 °C it gave cubic HgS with particle size of 26 nm and 34 nm (from the Scherrer formula[33]), respectively.

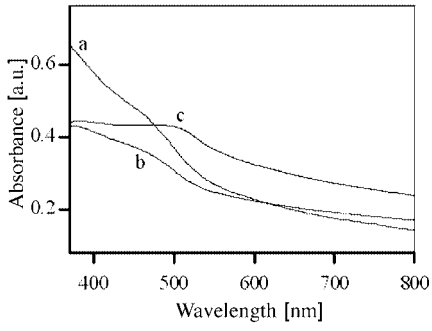

Figure 8. Absorption spectra of CdS nanoparticles obtained by the pyrolysis of $[Cd(S_2CPh)_2(tmeda)]$ with precursor: coordinating solvent mole ratio a) 1:34 (188 °C), b) 1:55 (188 °C) and c) 1:55 (225 °C).

Thermolysis of **3c** in HDA at 188, 188 and 225 °C having precursor/solvent mol ratio of 1:34, 1:55 and 1:55, respectively, gave nanoparticles of hexagonal CdS with different particle sizes. At fixed precursor/solvent mol ratio and duration, particle size increases with increase of temperature. This may be due to the growth of particles that accelerates with increasing temperature.[37] Thermolysis at a fixed duration and temperature with different precursor/solvent mol ratio 1:34 (particle size is 17 nm) and 1:55 (particle size is 26 nm) also gave different particle sizes which may be due to Ostwald ripenening.[38]

Electron Microscopy

The Selected Area Electron Diffraction (SAED) patterns of MS nanoparticles (Figure 9; Figures S5–S6 in the Supporting Information) obtained by pyrolysis of $[M(S_2CPh)_2(tmeda)]$ in a furnace at 350 °C for M = Zn, and in ethylenediamine for M = Cd (122 °C) and Hg (57 °C) revealed the formation of crystalline material. The diffraction rings in the SAED pattern of ZnS corresponds to the lattice planes (111), (220) and (311) which are assigned for the cubic phase. Concentric rings in the SAED patterns of MS (M = Cd or Hg) have been attributed to the lattice planes (100), (002), (101), (102), (110), (103) and (112) (CdS); (101), (102), (110), (104) and (105) (HgS), respectively, of the hexagonal phases of MS. The phases determined from the SAED and XRD patterns are in agreement. The TEM image of MS showed that ZnS nanoparticles [Figure S5 (Supporting Information)] are spherical in shape with an average diameter of 10 nm, while those of CdS (Figure 9) and HgS (Figure S6, Supporting Information) are nearly spherical with the average size of 20 and 25 nm, respectively. However, in the case of CdS, the presence of a small amount of nanorods of 20–60 nm in length and diameter of 12–20 nm

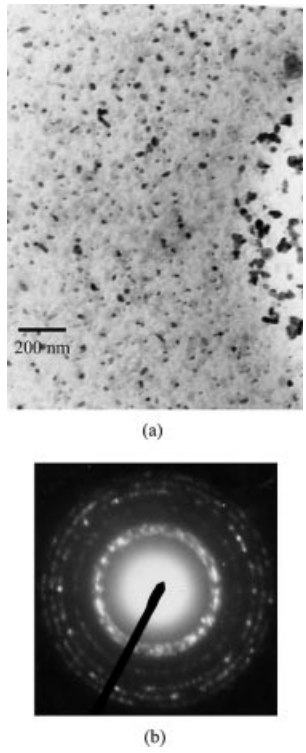

Figure 9. a) TEM image and b) SAED pattern of CdS nanoparticles obtained by pyrolysis of $[Cd(S_2CPh)_2(tmeda)]$ in ethylenediamine at 122 °C. In b) the inner ring is assigned to planes (100), (002) and (101), with the remaining rings from inner to outer corresponding to planes (102), (110), (103) and (112), respectively.

was also observed. Co-formation of nanoparticles of different morphology is known and optimization of reaction conditions can lead to the preferential deposition of one form over another.[39] The particle sizes of ZnS and HgS nanoparticles obtained from TEM images are in agreement with the sizes estimated from XRD pattern using the Scherrer formula,[33] whereas the sizes evaluated by these techniques differs for CdS nanoparticles. This inconsistency could be due to the deviation from spherical morphology of the CdS particles.[40]

Conclusions

Zinc, cadmium and mercury dithiocarboxylate complexes are conveniently prepared in high yields and are stable at room temperature for several months. The homoleptic derivatives are associated in the solid state and are sparingly soluble in non-coordinating solvents. The complexes with neutral donor ligands (e.g., py or tmeda) are discrete monomers. These complexes undergo facile decomposition both in the solid state (furnace heating) and in solution (solvothermal) to yield metal sulfide nanoparticles. The solvothermal decomposition affords nanoparticles at moderately low temperatures which can be as low as 57 °C for the preparation of HgS. Different phases (cubic/hexagonal) can be obtained under different experimental conditions. Thus, owing to the synthetic ease and facile conversion into phase pure metal sulfide nanoparticles, these complexes prove to be reliable precursors for the generation of MS, M = Zn, Cd and Hg.

Experimental Section

General: Elemental analyses were carried out by Radio Chemistry Division of B.A.R.C. ^{1}H and ^{13}C{^{1}H} NMR spectra were recorded with a Bruker DPX-300 NMR spectrometer operating at 300 and 75.47 MHz, respectively. Chemical shifts are relative to internal chloroform resonances at δ = 7.26 ppm for ^{1}H and δ = 77.0 ppm for ^{13}C{^{1}H}. UV/Vis absorption spectra were recorded with a Chemito Spectrascan UV 2600 double beam UV/Vis spectrophotometer. Fluorescence spectra were recorded using a Hitachi F-4500 FL spectrofluorometer.

Thermogravimetric analyses (TGA) were carried out with a Nitzsch STA PC-Luxx TG-DTA instrument, which was calibrated with $CaC_2O_4{\cdot}H_2O$. TG curves were recorded at a heating rate of 5 °C min^{-1} under a flow of nitrogen. Solvents were dried and distilled before use under nitrogen. HPLC-grade toluene was used in all experiments involving HDA as a capping agent while methanol was used in case of ethylenediamine as the capping agent. Dimethylformamide was used in pyrolysis experiments for optical studies. X-ray powder diffraction patterns were measured using Cu-K_α radiation with a Philips PW1820 powder diffractometer. EDAX were carried out with a Tescan Vega 2300T/40 instrument. A JEOL-2000FX transmission electron microscope operating at accelerating voltages up to 200 kV was used for TEM studies. The samples for TEM and SAED were prepared by placing a drop of sample dispersed in acetone on a carbon-coated copper grid.

Materials: Zinc, cadmium and mercury acetates, *N*,*N*,*N*′,*N*′-tetramethylethylenediamine (tmeda), hexadecylamine (HDA) and ethylenediamine (en), solvents were obtained from commercial sources. [M(OAc)$_2$(tmeda)] (M = Zn, Cd and Hg) were prepared by refluxing metal acetates with an excess of tmeda in dichloromethane under an inert atmosphere for 2 h. Dithiocarboxylic acids, RCS_2H (R = Ph, *p*-Tol) [NMR in $CDCl_3$ for R = Ph, ^{1}H NMR: δ = 6.40 (br. s, SH), 7.39 (br., 2 H, 3,5-H), 7.57 (br., 1 H, 4-H), 8.07 (br., *J* = 8.2 Hz, 2 H, 2,6-H) ppm. ^{13}C{^{1}H} NMR: δ = 126.7 (C-3,5), 128.2 (C-4), 133.0 (C-2,6), 143.5 (C-1), 225.2 (CS_2) ppm. ^{1}H NMR for R = *p*-Tol: δ = 2.38 (s, *Me*-tol), 4.71 (s, SH), 7.19 (d, *J* = 8.3 Hz, 2 H, 3,5-H), 7.98 (d, *J* = 8.2 Hz, 2 H, 2,6-H) (C_6H_4) ppm. ^{13}C{^{1}H} NMR: δ = 21.5 (Me), 126.9 (C-2,6), 129.0 (C-3,5), 141.1 (C-4), 144.2 (C-1), 224.6 (CS_2) ppm] were prepared by the reaction of RMgBr with CS_2 in diethyl ether as described in the literature method.[41]

Preparation of [Zn(S$_2$CTol)$_2$] (1a): A methanolic solution of $Zn(OAc)_2{\cdot}2H_2O$ (390 mg, 1.78 mmol) was added to a benzene solution (20 mL) of HS_2CTol (600 mg, 3.56 mmol), with vigorous stirring which continued for 2 h under nitrogen. The solvents were evaporated under vacuum to afford an orange residue (660 mg, 93%), m.p. 175 °C. $C_{16}H_{14}S_4Zn$ (399.94): calcd. C 48.0, H 3.5, S 32.1; found C 47.5, H 3.4, S 32.6. UV/Vis (CH_2Cl_2): λ = 334, 350 and 392 nm. ^{1}H NMR ($CDCl_3$): δ = 2.43 (s, C*H*$_3$C$_6$H$_4$CS$_2$), 7.22 (d, 7.5 Hz, C_6H_4), 8.28 (d, 7.5 Hz, C_6H_4) ppm. A portion of the residue was recrystallized as red crystals from dichloromethane containing few drops of pyridine. The ^{1}H NMR spectrum of these crystals, [Zn(S$_2$CTol)$_2$(py)] (**2**), showed resonances due to coordinated pyridine: ^{1}H NMR: δ = 2.73 (s, C*H*$_3$C$_6$H$_4$CS$_2$), 7.15 (d, *J* = 7.7 Hz, C_6H_4), 7.70 (d, *J* = 7 Hz, C_6H_4), 7.31 (br.), 8.38 (br.), 8.64 (br., py); this formulation was confirmed by an X-ray crystallographic study for red crystals grown by the slow evaporation of a dichloromethane solution of the compound.

Preparation of [Cd(S$_2$CTol)$_2$] (1b): This was prepared in a manner similar to the zinc complex in 92% yield as a red-orange crystalline solid; m.p. 160 °C. $C_{16}H_{14}CdS_4$ (446.96): calcd. C 43.0, H 3.2, S 28.7; found C 43.0, H 3.1, S 29.4. UV/Vis (CH_2Cl_2): λ = 321, 345, 360 nm. ^{1}H NMR ($CDCl_3$): δ = 2.37 (s, C*H*$_3$C$_6$H$_4$CS$_2$), 7.12 (br., *C*$_6$*H*$_4$), 8.30 (br., C_6H_4) ppm.

Preparation of [Zn(S$_2$CTol)$_2$(tmeda)] (3b): Solid [Zn(OAc)$_2$(tmeda)] (590 mg, 1.97 mmol) was added to a benzene solution (20 mL) of HS_2CTol (660 mg, 3.92 mmol), with vigorous stirring, which continued for 2 h under nitrogen. The solvent was removed under vacuum to yield an orange residue which was recrystallzed from dichloromethane/toluene (1:3) mixture to give red crystals (930 mg, 91% yield), m.p. 173 °C. $C_{22}H_{30}N_2S_4Zn$ (516.14): calcd. C 51.2, H 5.9, N 5.4, S 24.9; found C 51.3, H 5.9, N 5.4, S 25.0. UV/Vis (CH_2Cl_2): λ = 307, 326, 366 nm. ^{1}H NMR ($CDCl_3$): δ = 2.35 (s, C*H*$_3$C$_6$H$_4$CS$_2$), 2.62 (s, NMe_2), 2.70 (s, NCH_2), 7.10 (d, *J* = 7.4 Hz, C_6H_4), 8.36 (d, *J* = 7.3 Hz, C_6H_4) ppm. ^{13}C{^{1}H} NMR ($CDCl_3$): δ = 21.4 (*C*H$_3$-C$_6$H$_4$CS$_2$), 46.2 (NMe_2), 56.9 (NCH_2), 127.2, 128.1, 128.7, 142.7 (C_6H_4), 245.0 (C=S) ppm. Red crystals for X-ray diffraction were grown by the slow evaporation of a dichloromethane/toluene (3:1) solution of the compound.

Preparation of [Zn(S$_2$CPh)$_2$(tmeda)] (3a): This was prepared in a manner similar to [Zn(S$_2$CTol)$_2$(tmeda)] and recrystallized from dichloromethane/toluene as dark-red crystals in 92% yield, m.p. 152 °C (dec). $C_{20}H_{26}N_2S_4Zn$ (488.08): calcd. C 49.2, H 5.4, N 5.7, S 26.3; found C 49.5, H 5.4, N 5.9, S 25.7. UV/Vis (CH_2Cl_2): λ = 302, 366 nm. ^{1}H NMR ($CDCl_3$): δ = 2.65 (s, NMe_2), 2.73 (s, NCH_2), 7.30 (t, *J* = 7.7 Hz), 7.47 (t, *J* = 7.2 Hz), 8.44 (d, *J* = 7.4 Hz, Ph) ppm. ^{13}C{^{1}H} NMR ($CDCl_3$): δ = 46.1 (NMe_2), 56.7 (NCH_2), 126.9, 127.3, 131.7, 145.4 (Ph), 245.9 (C=S) ppm. Red crystals for X-ray crystallography were grown by the slow evapora-

tion of a dichloromethane/toluene (3:1) solution of the compound.

Preparation of [Cd(S_2CPh)$_2$(tmeda)] (3c): This complex was prepared in a similar fashion to its zinc analog and recrystallized from dichloromethane/hexane or dichloromethane/toluene mixture as orange crystals in 90% yield; m.p. 164 °C (dec). $C_{20}H_{26}CdN_2S_4$ (535.11): calcd. C 44.9, H 4.9, N 5.2, S 24.0; found C 45.4, H 4.8, N 4.8, S 24.5. UV/Vis (CH_2Cl_2): λ = 304, 368 nm. ^{1}H NMR ($CDCl_3$): δ = 2.60 (s, NMe_2), 2.69 (s, NCH_2), 7.32 (t, J = 7.8 Hz), 7.48 (t, J = 7.3 Hz), 8.47 (d, J = 7.7 Hz) (Ph) ppm. ^{13}C{^{1}H} NMR ($CDCl_3$): δ = 46.0 (NMe_2), 56.7 (NCH_2), 127.3, 128.2, 131.9, 145.4 (Ph), 249.0 (s, C=S) ppm. Red crystals for X-ray diffraction were grown by the slow evaporation of a chloroform/toluene (3:1) solution of the compound.

Preparation of [Cd(S_2CTol)$_2$(tmeda)] (3d): This was prepared similarly to [Zn(S_2CTol)$_2$(tmeda)] and recrystallized from dichloromethane/toluene in 90% yield as orange crystals; m.p. 176 °C. $C_{22}H_{30}CdN_2S_4$ (563.16): calcd. C 46.9, H 5.4, N 5.0, S 22.8; found C 47.3, H 5.4, N 5.1, S 23.0. UV/Vis (CH_2Cl_2): λ = 316, 328, 376 nm. ^{1}H NMR ($CDCl_3$): δ = 2.37 (s, CH_3C$_6$H$_4$CS$_2$), 2.57 (s, NMe_2), 2.66 (s, NCH_2), 7.10 (d, J = 7.8 Hz, C_6H_4), 8.39 (d, J = 7.8 Hz, C_6H_4) ppm. ^{13}C{^{1}H} NMR ($CDCl_3$): δ = 21.4 (*C*H$_3$-C$_6$H$_4$CS$_2$), 46.0 (NMe_2), 57.0 (NCH_2), 127.7, 128.1, 142.9, 143.4 (Ph), 248.4 (C=S) ppm.

Preparation of [Hg(S_2CPh)$_2$(tmeda)] (3e): The complex was obtained as a brown solid similarly to the previous mercury complex in 90% yield; m.p. 78 °C (dec). $C_{20}H_{26}HgN_2S_4$ (623.29): calcd. C 38.5, H 4.2, N 4.5, S 20.6; found C 37.9, H 3.7, N 4.3, S 21.2. UV/Vis (CH_2Cl_2): λ = 298 (sh), 310 nm. ^{1}H NMR ($CDCl_3$): δ = 2.43 (s, NMe_2), 2.66 (s, NCH_2), 7.38 (t, J = 7 Hz), 7.56 (t, J = 7.2 Hz), 8.19 (br., Ph) ppm. ^{13}C{^{1}H} NMR ($CDCl_3$): δ = 45.2 (NMe_2), 56.2 (NCH_2), 126.9, 127.9, 132.7, 144.3 (Ph) ppm; the resonance due to C=S was not resolved.

Preparation of [Hg(S_2CTol)$_2$(tmeda)] (3f): This was prepared similarly to its zinc, cadmium analogs as a brown solid in 91%; m.p. 112 °C. $C_{22}H_{30}HgN_2S_4$ (651.34): calcd. C 40.6, H 4.6, N 4.3, S 19.7; found C 40.1, H 4.1, N 4.0, S 20.3. UV/Vis (CH_2Cl_2): λ = 315, 335, 361 nm. ^{1}H NMR ($CDCl_3$): δ = 2.39 (s, NMe_2), 2.38 (s, CH_3C$_6$H$_4$CS$_2$), 2.57 (s, NCH_2), 7.16 (d, J = 7.7 Hz, C_6H_4), 8.15 (br., C_6H_4) ppm.

X-ray Crystallography: Intensity data for [Zn(S_2CTol)$_2$(py)], [Zn(S_2CTol)$_2$(tmeda)], [Zn(S_2CPh)$_2$(tmeda)] and [Cd(S_2CTol)$_2$-(tmeda)] were measured with a Rigaku AFC12/Saturn724 CCD fitted with Mo-K_α radiation so that θ = 27.5°. The structures were solved by heavy-atom methods[42] and refinement was on F^2 [43] using data that had been corrected for absorption effects with an empirical procedure,[44] with non-hydrogen atoms modeled with anisotropic displacement parameters, with hydrogen atoms in their calculated positions, and using a weighting scheme of the form $w = 1/[\sigma^2(F_o^2) + (aP)^2 + bP]$ where $P = (F_o^2 + 2F_c^2)/3$. The absolute configuration of [M(S_2CTol)$_2$(tmeda)], M = Zn and Cd, was determined on the basis of differences in Friedel pairs included in the data sets and confirmed by the near-zero value of the Flack parameter in each case, i.e. 0.006(12) and –0.01(3), respectively.[45] A residual electron density peak of 2.02 e Å^{-3} was noted in the final difference map for [Zn(S_2CPh)$_2$(tmeda)], this was located between the Zn and S1 atoms. A residual of 1.05 e Å^{-3} was located 0.02 Å from the Cd atom in [Cd(S_2CTol)$_2$(tmeda)]. Molecular structures shown in Figures 1, 2, 3, and 4 were drawn at the 50% probability level using ORTEP.[46] The DIAMOND program[47] was used for the remaining crystallographic figures. Data manipulation and analyses were performed with teXsan[48] and PLATON.[49] Crystallographic data and refinement details are given in Table 1.

Preparation of Metal Sulfide Nanoparticles

(a) Pyrolysis in a Furnace: A weighed quantity of a sample (ca. 200 mg) in a quartz boat, was pyrolyzed at 350 °C (unless otherwise stated) in a furnace under flowing nitrogen for 2 h. After cooling, the residue in the quartz boat was again weighed and characterized by XRD and in some cases by UV/Vis spectroscopy. The pyrolysis of **3c** was carried out at three different temperatures, 300, 400 and 500 °C and the dark-red residual powder was characterized by XRD.

Table 1. Crystallographic parameters and refinement details for [Zn(S_2CTol)$_2$(py)], [Zn(S_2CTol)$_2$(tmeda)], [Zn(S_2CPh)$_2$(tmeda)] and [Cd(S_2CTol)$_2$(tmeda)].

Parameter	[Zn(S_2CTol)$_2$·py]	[Zn(S_2CTol)$_2$(tmeda)]	[Zn(S_2CPh)$_2$(tmeda)]	[Cd(S_2CTol)$_2$(tmeda)]
Formula	$C_{21}H_{19}NS_4Zn$	$C_{22}H_{30}N_2S_4Zn$	$C_{20}H_{26}N_2S_4Zn$	$C_{22}H_{30}CdN_2S_4$
Fw	478.98	516.09	488.04	563.12
Crystal system	monoclinic	orthorhombic	monoclinic	orthorhombic
Space group	*C*2/*c*	*Aba*2	*C*2/*c*	*Aba*2
a [Å]	17.451(6)	13.140(3)	18.419(4)	12.644(3)
b [Å]	9.023(2)	23.098(5)	8.0230(16)	23.859(5)
c [Å]	13.979(4)	7.8304(15)	15.404(3)	7.9794(16)
β [°]	107.038(6)	90	98.251(4)	90
V [Å^3]	2104.6(11)	2376.6(8)	2252.9(8)	2407.1(9)
Z	4	4	4	4
μ [cm^{-1}]	1.570	1.397	1.469	1.266
$D_{calcd.}$ [g cm^{-3}]	1.512	1.442	1.439	1.554
Independent reflections	2412	2720	2582	2741
Observed reflections with $I > 2\sigma(I)$	2340	2677	2506	2717
R (obsd. data)	0.049	0.034	0.054	0.026
a, *b* in weighting scheme	0.065, 5.371	0.052, 1.787	0.042, 42.646	0.031, 4.477
R_w (all data)	0.127	0.084	0.160	0.062
CCDC numbers[a]	616718	616716	616717	616715

[a] The supplementary crystallographic data for this paper can be obtained free of charge from The Cambridge Crystallographic Data Centre (CCDC) via www.ccdc.cam.ac.uk/data_request/cif.

(b) Preparation of MS (M = Zn, Cd, Hg) Nanoparticles in Coordinating Solvents: All experiments were performed similarly. A typical experiment is described below:

In a three-necked flask fitted with a thermometer, HDA (hexadecylamine) (5 g) was degassed at 120 °C under argon for 1 h with continuous stirring. The temperature was slowly raised to 225 °C and stabilized at this temperature. To this, a solution of **3c** (200 mg, 0.37 mmol) in dichloromethane (3 mL) was injected rapidly. The temperature dropped to 195 °C and was slowly raised to 225 °C and maintained at this temperature for 10 min. This hot solution was maintained at 225 °C for 20 min and was cooled to 70 °C and methanol was added to precipitate yellow CdS nanoparticles. The yellow flocculate was given a thorough washing with methanol followed by centrifuging and drying under vacuum.

Similarly, experiments were carried out at different temperatures and at different concentrations of precursor and coordinating solvent. Metal sulfide nanoparticles prepared in ethylenediamine were isolated by centrifuging rather than precipitating with methanol. The particles thus separated were thoroughly washed with methanol and dried. In case of experiments performed in ethylenediamine, a sudden surge in temperature to 135–140 °C was observed when the precursor (zinc, cadmium and mercury) was injected at 115 °C into ethylenediamine.

Supporting Information (see also the footnote on the first page of this article): XRD slides of nanoparticles of different colors, SAED patterns and TEM images of ZnS, HgS nanoparticles.

Acknowledgments

We thank Drs. T. Mukherjee and S. K. Kulshreshtha for encouragement of this work. The authors are grateful to Dr. S. K. Gupta and his group for EDAX measurements and Dr. V. K. Manchanda and his group for providing microanalysis of these complexes.

[1] a) H. S. Nalwa, Encyclopedia of Nanoscience and Nanotechnology (Eds.: P. Reiss, A. Pron), American Scientific Publishers, USA, vol. 6, **2004**, 587–604; b) A. P. Alivisatos, *Science* **1996**, *271*, 933–937.
[2] V. L. Colvin, M. C. Schlamp, A. P. Alivisatos, *Nature* **1994**, *370*, 354–357.
[3] V. I. Klimov, A. A. Mikhailovsky, S. Xu, A. Malko, J. A. Hollingsworth, C. A. Leatherdale, H.-J. Eisler, M. G. Bawendi, *Science* **2000**, *290*, 314–317.
[4] S. Coe, W. K. Woo, M. G. Bawendi, V. Bulovic, *Nature* **2002**, *420*, 800–803.
[5] W. U. Huynh, J. J. Dittmer, A. P. Alivisatos, *Science* **2002**, *295*, 2425–2427.
[6] http://www.nrel.gov/ncpv/ncpv.html.
[7] M. Green, *Angew. Chem. Int. Ed.* **2004**, *43*, 4129–4131.
[8] W. C. W. Chan, S. M. Nie, *Science* **1998**, *281*, 2016–2018.
[9] P. V. Braun, P. Osenar, S. I. Stupp, *Nature* **1996**, *380*, 325–328.
[10] T. Trindade, P. O'Brien, N. L. Pickett, *Chem. Mater.* **2001**, *13*, 3843–3858.
[11] O. Masala, R. Seshadri, *Annu. Rev. Mater. Res.* **2004**, *34*, 41–81.
[12] a) M. Yosef, A. K. Schaper, M. Froba, S. Schlecht, *Inorg. Chem.* **2005**, *44*, 5890–5896; b) Y. W. Jun, J. E. Koo, J. Cheon, *Chem. Commun.* **2000**, 1243–1244.
[13] a) M. D. Nyman, M. J. Hampden-Smith, E. N. Duesler, *Adv. Mater. CVD* **1996**, *5*, 171–174; b) M. D. Nyman, M. J. Hampden-Smith, E. N. Duesler, *Inorg. Chem.* **1997**, *36*, 2218–2224.
[14] Z. H. Zhang, W. S. Chin, J. J. Vittal, *J. Phys. Chem. B* **2004**, *108*, 18569–18574.
[15] G. Kedarnath, L. B. Kumbhare, V. K. Jain, P. P. Phadnis, M. Nethaji, *Dalton Trans.* **2006**, 2714–2718.
[16] J. Cheon, D. S. Talaga, J. I. Zink, *J. Am. Chem. Soc.* **1997**, *119*, 163–168.
[17] D. Barreca, A. Gasparotto, C. Maragno, R. Seraglia, E. Tondello, A. Venzo, V. Krishnan, H. Bertagnolli, *Appl. Organomet. Chem.* **2005**, *19*, 59–67.
[18] a) M. Motevalli, P. O'Brien, J. R. Walsh, *Polyhedron* **1996**, *15*, 2801–2808; b) M. Lazell, P. O'Brien, *Chem. Commun.* **1999**, 2041–2042; c) M. Chunggaze, M. A. Malik, P. O'Brien, *J. Mater. Chem.* **1999**, *9*, 2433–2438.
[19] Y. W. Jun, S. Min Lee, N.-J. Kang, J. Cheon, *J. Am. Chem. Soc.* **2001**, *123*, 5150–5151.
[20] C. Byron, M. A. Malik, P. O'Brien, A. P. J. White, D. J. Williams, *Polyhedron* **2000**, *19*, 211–215.
[21] I. Haiduc, D. B. Sowerby, S. F. Lu, *Polyhedron* **1995**, *14*, 3389–3472.
[22] G. Hogarth, *Prog. Inorg. Chem.* **2005**, *53*, 71–561.
[23] E. R. T. Tiekink, I. Haiduc, *Prog. Inorg. Chem.* **2005**, *54*, 127–319.
[24] E. R. T. Tiekink, *CrystEngComm* **2003**, *5*, 101–113.
[25] M. Bonamico, G. Dessy, V. Fares, L. Scaramuzza, *J. Chem. Soc., Dalton Trans.* **1972**, 2515–2517.
[26] D. J. Darensbourg, M. J. Adams, J. C. Yarbrough, *Inorg. Chem. Commun.* **2002**, *5*, 38–41.
[27] H. Adams, A. C. Albeniz, N. A. Bailey, D. W. Bruce, A. S. Cherodian, R. Dhillon, D. A. Dunmer, P. Espinet, J. L. Feijoo, E. Lalinde, P. M. Maitlis, R. M. Richardson, G. Ungar, *J. Mater. Chem.* **1991**, *1*, 843–856.
[28] a) N. Kano, T. Kawashima, *Top. Curr. Chem.* **2005**, *251*, 141–180; b) C. Furlani, M. L. Luciani, *Inorg. Chem.* **1968**, *7*, 1586–1592.
[29] A. W. Addison, T. N. Rao, J. Reedijk, J. van Rijn, G. C. Verschoor, *J. Chem. Soc., Dalton Trans.* **1984**, 1349–1356.
[30] *International Center for Diffraction data*, JCPDS File No. 80–0020, **1997**.
[31] *International Center for Diffraction data*, JCPDS File No. 75–1538, **1997**.
[32] *International Center for Diffraction data*, JCPDS File No. 77–2306, **1997**.
[33] a) B. D. Cullity, *Elements of X-ray diffraction*, Addison-Wesley Inc., London, **1978**; b) N. Bhatt, R. Vaidya, S. G. Patel, A. R. Jani, *Bull. Mater. Sci.* **2004**, *27*, 23–25.
[34] J. Z. Zhang, *J. Phys. Chem. B* **2000**, *104*, 7239–7253.
[35] Y. Jun, J. Lee, J. Choi, J. Cheon, *J. Phys. Chem. B* **2005**, *109*, 14795–14806.
[36] *International Center for Diffraction data*, JCPDS File No. 06–0256, **1997**.
[37] C. B. Murray, D. J. Norris, M. G. Bawendi, *J. Am. Chem. Soc.* **1993**, *115*, 8706–8715.
[38] X. Peng, J. Wieckham, A. P. Alivisatos, *J. Am. Chem. Soc.* **1998**, *120*, 5343–5344.
[39] P. S. Nair, G. D. Scholes, *J. Mater. Chem.* **2006**, *16*, 467–473.
[40] P. S. Nair, T. Radhakrishnan, N. Revaprasadu, G. A. Kolawole, P. O'Brien, *Chem. Commun.* **2002**, 564–565.
[41] a) P. Beslin, A. Dlubala, G. Levesue, *Synthesis* **1987**, 835–837; b) R. W. Bost, W. J. Mattox, *J. Am. Chem. Soc.* **1930**, *52*, 332–335.
[42] P. T. Beurskens, G. Admiraal, G. Beurskens, W. P. Bosman, S. García-Granda, J. M. M. Smits, C. Smykalla, *The DIRDIF program system*, Technical Report of the Crystallography, Laboratory, University of Nijmegen, Nijmegen, The Netherlands, **1992**.
[43] G. M. Sheldrick, *SHELXL97*. Program for crystal structure refinement. University of Göttingen, Germany, **1997**.
[44] T. Higashi, *ABSCOR*, Empirical Absorption Correction based on Fourier Series Approximation, Rigaku Corporation, 3-9-12 Matsubara, Akishima, Japan, **1995**.

[45] H. D. Flack, *Acta Crystallogr., Sect. A* **1983**, *39*, 876–881.
[46] C. K. Johnson, *ORTEP II*, Report ORNL-5136, Oak Ridge National Laboratory, Oak Ridge, TN, **1976**.
[47] *Crystal Impact*, *DIAMOND*, *Version 3.1*. Crystal Impact GbR, Postfach 1251, 53002 Bonn, Germany, **2006**.
[48] *teXsan*, Structure Analysis Package, Molecular Structure Corporation, Houston, TX, **1992**.
[49] A. L. Spek, *PLATON*, A Multipurpose Crystallographic Tool, Utrecht University, Utrecht, The Netherlands, **2006**.
Received: November 12, 2006
Published Online: March 6, 2007

